

Molecular Mechanics Force Field for Octahedral Organometallic Compounds with Inclusion of the Trans Influence

Ivan Tubert-Brohman, Maurus Schmid, and Markus Meuwly*

University of Basel, Klingelbergstrasse 80, 4052 Basel, Switzerland

Received September 19, 2008

Abstract: Efficient calculation of the properties of metal-containing complexes relevant to catalysis is of major interest for better characterizing and optimizing the catalysts. For this, a new force field, called VALBOND-TRANS here, is proposed. It is based on the existing VALBOND force field of Landis and co-workers, extended by adding terms that account for electronic effects such as the trans influence of ligands on bond lengths and relative energies. Parameters and results for model octahedral complexes of Ru, Os, Rh, and Ir are determined and discussed. The model is then applied to the study of reactive intermediates involved in asymmetric hydrogenation catalyzed by iridium complexes with chiral phosphinoxazolines (PHOX) ligands. The new force field explores and capitalizes on the separation of electronic and steric effects on the stability of different diastereomers and reproduces DFT results which are consistent with experimental observations.

1. Introduction

Theoretical methods can be very helpful for understanding and predicting structure and reactivity in organometallic chemistry. Density functional theory (DFT) methods, in particular, have been very successful for the computational study of transition metal complexes.¹ However, DFT calculations are CPU-intensive, which makes the treatment of large complexes difficult. Such calculations are often limited to geometry optimizations of gas-phase structures or to model systems with smaller and sometimes unrealistic ligands. Dynamics simulations and calculations over large libraries of compounds are often impractical. Therefore, having a faster, even if approximate method is desirable. Molecular mechanics (MM) force fields such as OPLS,² AMBER,³ and CHARMM⁴ have become standard methods in biomolecular chemistry and are routinely used for molecular dynamics simulations of systems with up to 1 million atoms.⁵ However, the development of general force fields for transition metal complexes has been relatively limited because of the unique difficulties presented by these types of compounds:^{6–15} metals can have a variety of coordination numbers, π -binding ligands can bind in various ways, and electronic effects such

as the Jahn–Teller distortion and the trans influence need to be considered. Although considerable work has been done toward including the Jahn–Teller distortion in molecular mechanics,^{16,17} the molecular mechanics of the trans influence remains largely unexplored. Here, we present a model for the trans influence and implement it in a force field for octahedral complexes of iridium and three other platinum-group metals (Ru, Os, and Rh). We then test our method on real complexes relevant to asymmetric hydrogenation. The current work is a conventional force field in the sense that it does not allow the formation and breaking of bonds, which are essential for the modeling of chemical reactions. This work, however, can be readily combined with the adiabatic reactive molecular dynamics (ARMD) approach recently developed by our group.¹⁸ In ARMD, a conventional force field description of the reactants and products is used for each dynamics time step, and the system is propagated along the lower energy state, with specific rules for treating crossover between the reactant and product states.

Asymmetric hydrogenation is one of the most important catalytic methods for the preparation of optically active compounds, both in the laboratory and in industry.¹⁹ Iridium catalysts with chiral N,P ligands are a class of highly efficient catalysts that have expanded the scope of asymmetric

* Corresponding author e-mail: m.meuwly@unibas.ch.

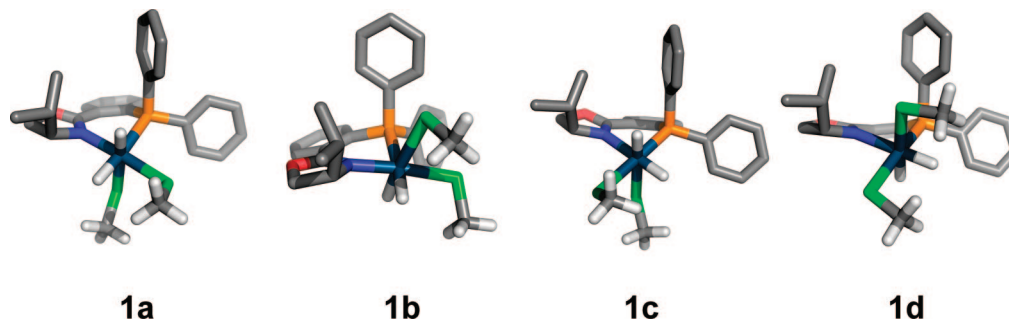


Figure 1. DFT-calculated structures of $[\text{Ir}(\text{PHOX})(\text{H})_2(\text{CH}_3\text{Cl})_2]^+$ complexes.²⁴

hydrogenation to include unfunctionalized alkenes.^{19–23} In a recent study, we used DFT calculations in combination with NMR data to show that the hydrogenation reaction may proceed through dihydride intermediates **1a–1d** (Figure 1).²⁴ Here we revisit these compounds to see whether it is possible to capture the necessary electronic effects within a force field representation that can also be extended to other related compounds.

VALBOND, developed by Landis and co-workers, is a force field that computes the angle bending energies based on valence bond theory.²⁵ Its main premise is that the bending energy is a function of the overlap of the hybrid orbitals on the central atom, using hybridizations that are computed using certain rules. Unlike the simple harmonic approximation used by many force fields for the bending potential, the VALBOND bending function gives reasonable results at very large distortions. VALBOND also supports hypervalent compounds by means of a 3-center-4-electron bonding model.²⁶ As a result, it can describe geometries found in organometallic compounds, such as octahedral, trigonal bipyramidal, and square planar. VALBOND has been shown to work for transition metal compounds of a largely covalent nature, such as hydrides and alkyls.²⁷ For these compounds, VALBOND uses a 12-electron rule, where only *sd* hybrids are considered, and excess electrons are involved in hypervalent bonds. In order to have a complete force field, VALBOND has to be combined with another force field such as CHARMM⁴ or UFF,²⁸ to account for the bond stretching, torsional, and nonbonded energy terms. VALBOND does not account for the trans influence, but the valence bond ideas behind the force field led us to investigate a plausible way of incorporating it.

Another approach to the molecular mechanics of coordination compounds is the inclusion of force field terms corresponding to the ligand field stabilization energy, as done in the ligand field molecular mechanics (LFMM) model of Deeth and co-workers¹⁷ and the SIBFA-LF method of Gresh and co-workers.²⁹ The LFMM method has been applied to Werner-type complexes of Cu^{2+} , Ni^{2+} , Co^{3+} , and Mn^{2+} ; it is able to account for a number of coordination geometries and for the Jahn–Teller effect and can also incorporate the contribution of the *s* orbitals that is important for complexes such as WH_6 and $[\text{CuCl}_4]^{2-}$. LFMM has also been successfully applied to the study of type I copper proteins.³⁰ However, we chose VALBOND for our work because it has been tested more extensively with compounds resembling the ones involved in catalytic hydrogenation, such as alkyl

and hydride complexes of metals from the second and third transition series.²⁷

The trans influence has been defined as “the tendency of a ligand to selectively weaken the bond trans to itself”.³¹ It is an electronic ground-state phenomenon, unlike the trans effect, which is defined in terms of the rate of a substitution reaction.³² Although much of the work on trans influences and trans effects has focused on square planar complexes, these effects are also important for octahedral complexes.³² Experimental studies of the trans influence generally concentrate on the lengthening of the trans bond as measured from crystallographic methods. The trans influence can also affect the relative stability of different diastereomers, but this has not been studied as extensively experimentally due to the difficulties of gathering thermochemical data for metal compounds.³³ For this reason, theoretical studies and molecular mechanics methods have often concentrated on the geometric influence. An early example is an MM3 study which found that the central nitrogen in terpyridine forms an unusually short Ru–N bond which causes the Ru–N bond trans to it to stretch; the authors simulated this effect within the force field by adding a pseudobond to constrain the N–N distance;³⁴ this is a case where the trans influence is caused not by the electronic nature of the ligand but by the strain caused by its tridentate nature. As a note on terminology, we use the terms *structural trans influence* to refer to the bond lengthening effect and *thermodynamic trans influence* to refer to the effect on the relative stability of different diastereomers.

We believe that current theoretical methods and computer power are ripe for a systematic study of the thermodynamic trans influence. The main goal of the present work is to explore the thermodynamic trans influence on the relative energies of different diastereomers of octahedral organometallic compounds and to implement a force field that can predict which isomers are most stable. We chose the octahedral geometry not only because of its ubiquity but also because of its rich stereochemistry: a complex with six different ligands has fifteen possible diastereomers, and predicting which one is most stable involves an intricate mix of steric and electronic effects. As a secondary goal, we also considered the geometric trans influence and incorporated it into our force field, but at this stage we were not concerned with spectroscopic properties or with using the most accurate possible functions and parameters for bond stretching and for bonding angles.

The current work is structured as follows. First, we review the theory underlying VALBOND and the trans influence and describe modifications and additions we envisage. Next, we describe the parametrization of the new method using a training set of simple model compounds. Then we present results for two test cases involving real complexes of relevance to asymmetric hydrogenation. Finally, general conclusions and suggestions for future developments are discussed.

2. Theory

Qualitatively, the trans influence may be attributed to the effect of different ligands on the resonance structures representing a 3-center-4-electron bond:^{35,36}



In this picture, the ligand that forms the stronger bond to the metal will weaken the bond to the weaker ligand. This leads to *antisymbiosis*, where “stronger” ligands prefer to bind trans to “weaker” ones, or softer ligands prefer to bind trans to harder ones.³⁷

Based on the idea of the trans influence acting through a 3-center-4-electron bond, a natural place for incorporating this effect into VALBOND is in the part of the algorithm that treats hypervalent molecules. Note that, under this model, the trans influence will only exist for hypervalent complexes; however, most transition metal complexes, including all octahedral and square complexes of groups 8–10 are hypervalent according to the VALBOND formalism, due to its use of the 12-electron rule instead of the 18-electron rule.

The VALBOND equations that are directly relevant to our modifications are eqs 2–4, below, which describe hypervalent bonding. For a detailed explanation and for the nonhypervalent VALBOND equations, the reader is referred to the original literature.^{25–27}

$$E(\alpha) = BOF \times k_{\alpha} (1 - \Delta(\alpha + \pi)^2) \quad (2)$$

$$\Delta = \frac{1}{1 + m + n} \left(1 + m \cos \alpha + \frac{n}{2} (3 \cos^2 \alpha - 1) \right) \quad (3)$$

$$c_i = \frac{\prod_{i=1}^{hype} \Delta_i^2}{\sum_{j=1}^{res} \prod_{i=1}^{hype} \Delta_i^2} \quad (4)$$

Here $E(\alpha)$ is the bending energy of a hypervalent bond, BOF is the bond order factor (always 0.25 for hypervalent bonds), α is the angle, k_{α} is a force constant, and Δ is the overlap between two orbitals with $sp^m d^n$ hybridization (Figure 2). VALBOND iterates over all possible resonance structures (*res*) that distribute the hypervalent bonds among the different ligands in different ways, giving each configuration i a weight c_i proportional to the product of Δ^2 over all hypervalent bonds (*hype*). The key equation is eq 2, which defines the bending energy of a 3-center-4-electron bond as proportional to the overlap between one orbital and another orbital shifted by 180° . This term favors linear geometries in hypervalent bonds, because $\Delta(\alpha + \pi) = 1$ when $\alpha = 180^\circ$, which leads to a minimum of $E(\alpha)$ at 180° . Because the trans influence

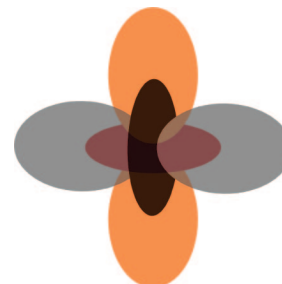


Figure 2. Cartoon representation of the overlap between two sd^2 orbitals at 90° . For normal bonds, the overlap is minimal at 90° , the equilibrium geometry. For hypervalent bonds, the equilibrium geometry corresponds to the maximum overlap at 180° .

also acts along hypervalent bonds and is expected to be maximal at 180° , it seems reasonable to include the $\Delta(\alpha + \pi)^2$ term from eq 2 in a function for representing the thermodynamic trans influence. A simple and efficient function that was successful in practice is

$$E_{trans} = \sum_{i=1}^{hype} p_{AB} \Delta(\alpha + \pi)^2 \quad (5)$$

where p_{AB} is an adjustable parameter which depends on the types of ligands and metal involved. These parameters are determined by least-squares fitting to DFT energies of model compounds. Eq 5, like eq 2, is used for each resonance configuration and weighed accordingly.

For the structural trans influence, preliminary tests showed that the bond lengths could best be fitted by a function of the type

$$r_{A(B)} = r_A^0 (1 + s_A \cdot i_B / 100) \quad (6)$$

where $r_{A(B)}$ is the equilibrium bond length of a bond from the metal to a ligand of type A which is trans to a ligand of type B, r_A^0 is the reference or unperturbed bond length to a ligand of type A, i_B is the “trans influence intensity” due to ligands of type B, and s_A is the “lengthening sensitivity” of bonds to ligands of type A. Like the trans influence on the energy, the trans influence on the bond length is implemented in the force field as part of the hypervalent bonding calculation and includes the overlap function as

$$r_{A(B)} = r_A^0 (1 + s_A \cdot \Delta(\alpha + \pi)^2 \cdot i_B / 100) \quad (7)$$

In the molecular mechanics calculations, $r_{A(B)}$ is used for the equilibrium bond length, r_0 , in the standard harmonic bond energy function, $E_{bond}(r) = k_B(r - r_0)^2$.

3. Parametrization

Thermodynamic Trans Influence. The model was parametrized against a training set comprising 129 series of diastereomers of octahedral complexes of Ru, Os, Rh, and Ir with oxidation states II and III, for a total of 532 structures (Table 1). Each series consists of all diastereomers of a given complex, ranging from two isomers for complexes of type MX_4Y_2 (cis/trans isomerism) and MX_3Y_3 (fac/mer isomerism), to up to fifteen diastereomers for complexes with six different ligands. The choice of

Table 1. Composition of the Training Set

	number of series	number of isomers
Ru(II)	20	60
Ru(III)	24	134
Os(II)	16	49
Os(III)	13	69
Rh(III)	24	86
Ir(III)	32	134
total	129	532

compounds in the training set was motivated by complexes from the Cambridge Structural Database³⁸ and from the review by Coe and Glenwright,³² with all ligands replaced with small model ligands: Cl^- , Br^- , H^- , H_2O , NH_3 , PH_3 , CH_3^- , CH_3OCH_3 , CH_3Cl , $\text{CH}_2=\text{CH}^-$, and C_6H_5^- . This truncation, in addition to speeding up the calculations, minimizes steric interactions between the ligands, which allows us to better focus on electronic effects. All the reference energies and structural data were obtained from B3LYP³⁹ calculations, which were carried out using GAUSSIAN 03,^{40,41} with the LANL2DZ effective core potential⁴² for the metals and the 6-31G(d,p) basis set for all other atoms. The grid=ultrafine option was used for consistency with previous work.²⁴

The DFT energy of each compound relative to the maximum energy isomer in its series was fit to the following function

$$\Delta E = \sum_{\text{trans}} p_{AB} \quad (8)$$

by means of a least-squares procedure. This function is equivalent to eq 5 for perfectly octahedral geometries. The relative energies used in the parametrization can be interpreted as energies of isomerization from the least stable isomer to a given isomer of a compound. For example, Figure 3 shows the series of compounds with formula $[\text{Ir}(\text{PH}_3)_3(\text{H})(\text{CH}_3)(\text{Cl})]$, along with their relative energies computed using eq 8 and the reference DFT values. For Ru and Os, which are found in two different oxidation states (II and III) in the training set, separate parameters were fitted for each oxidation state. Note, however, that the same parameters (“atom types”) were used for all carbon ligands (CH_3^- , $\text{CH}_2=\text{CH}^-$, and C_6H_5^-) and for all oxygen ligands (H_2O and CH_3OCH_3); the validity of this assumption will be scrutinized further below. Because only relative energies are of interest, a common zero of energy was chosen by setting all the parameters involving the chloride anion to zero. The resulting parameters together with their average errors are shown in Table 2. The 109 adjustable parameters were fitted to 403 relative energies, with an overall mean absolute deviation (MAD) of 1.31 kcal/mol and an rmsd of 1.78 kcal/mol. The correlation between the values calculated using eq 8 and the DFT data is shown in Figure 4. The linear regression is close to $y = x$ with $R^2 = 0.93$. Most of the isomerization energies are within a range of 25 kcal/mol; the four points between -40 and -30 kcal/mol all correspond to compounds with the CH_3Cl ligand, which binds very weakly and is particularly sensitive to the thermodynamic trans influence. When considering the values of the parameters, the antisymbiotic effect is especially noticeable

for hydride and methyl, which have a strong trans influence. Having H or C trans to H or C is unfavorable by up to 20 kcal/mol, relative to having them trans to chloride; conversely, having C or H trans to weaker trans-influencing ligands such as N and O is generally favorable, by up to -10 kcal/mol.

Although two different parameters were required for chlorine-binding ligands (one for the chloride ion and one for chloromethane), parameters for neutral oxygen ligands were found to be reasonably transferable—the same parameter can be used for water and for dimethyl ether as a ligand. Similarly, different carbon ligands are reproduced satisfactorily despite changes in hybridization and the addition of electron-donating or electron-withdrawing groups. As an illustration, Table 3 shows the isomerization energies for several series of nine compounds with formula $[\text{Ir}(\text{H})(\text{PH}_3)(\text{NH}_3)_2(\text{OH}_2)\text{R}]^+$, where R is a formally anionic carbon ligand. The same trend is followed for all the R ligands considered, with an overall mean absolute deviation of 0.9 kcal/mol.

A possible drawback of eq 8 is that, for N ligand types, up to $N(N-1)/2$ parameters are required per metal; that is, the number of parameters scales roughly as N^2 . It would be desirable to have atom-based parameters which scaled as N . We investigated functions such as $p_{AB} = p_A - p_B$, based on the idea of antisymbiosis,³⁷ but the results, while initially promising, were not sufficiently general for our purposes. Other simple functions such as $p_{AB} = p_A \cdot p_B$ were also tested with similar results.

Structural Trans Influence. The parameters in eq 6 were fit against all 2622 metal–ligand bond lengths in the training set using a least-squares method. The resulting parameters and average errors are summarized in Table 4. The overall mean absolute deviation is 0.019 Å (rmsd = 0.027 Å), which is less than one-tenth of the observed range of bond lengths for each bond type (for example, the ligands exerting the strongest trans influence, hydride and alkyl, can lengthen bonds trans to them by about 0.2 Å). The correlation between the predicted and the reference bond lengths is shown in Figure 5a. For comparison, a fit where the trans influence term is omitted, by setting i_B or s_A to zero, was also calculated; only the values of r^0 (not shown) were optimized for this comparison. This way we can compare our new approach with what would be the best possible result that can be obtained with a “constant r^0 ” approach. With the trans influence neglected, the mean absolute deviation increases to 0.044 Å (rmsd = 0.061 Å). The correlation between the bond lengths calculated without the trans influence and the reference values is shown in Figure 5b.

Examination of the structural trans influence parameters reveals a slight reciprocal correlation between intensity and sensitivity (correlation coefficient $R = 0.53$); this agrees with the analysis of the trans influence in terms of resonance structures discussed above, because ligands with a stronger trans influence will form bonds with a more covalent character, which can reasonably be expected to be less flexible than the more polar bonds formed with the weaker trans-influencing ligands. Another striking feature of the parameter values are the large differences between the para-

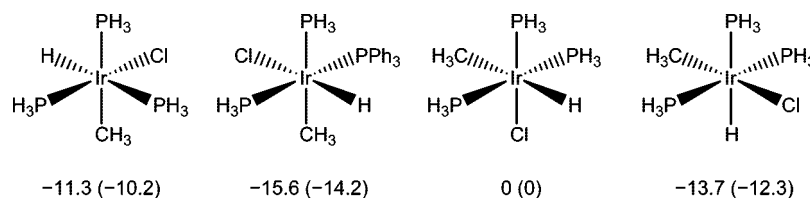


Figure 3. Isomers with formula $[\text{Ir}(\text{PH}_3)_3\text{HCH}_3\text{Cl}]$, with relative computed energies using eq 8 in kcal/mol (DFT values in parentheses).

Table 2. Parameters, Mean Absolute Deviation (MAD), and Root-Mean-Square Deviation (RMSD)^a

parameter	Ru(II)	Ru(III)	Os(II)	Os(III)	Rh(III)	Ir(III)
p_{BrBr}	0.30	-0.07	0.41	-1.34	0.54	3.35
p_{CBr}		0.19		-1.06	3.14	6.41
p_{CC}	5.95		4.32		20.61	18.61
p_{CH}		10.28		15.30	19.65	18.30
p_{CO}		-8.34		-7.50	-9.55	-6.16
p_{HH}	16.17		18.12		15.95	20.42
p_{NBr}	-0.54	-2.00		-1.12	0.67	2.28
p_{NC}	-4.64	-3.73	-5.79	-1.08	-3.68	-2.81
p_{NH}	-1.38	-3.67	0.15	3.92	-5.82	-4.27
p_{NN}	-6.46	-10.28	-7.77	-6.93	-8.88	-9.58
p_{NO}	-6.63	-8.18	-9.60	-5.20	-3.35	-5.50
p_{OBr}		-0.33		-1.47	-1.35	-0.14
p_{OH}	-9.26	-8.81	-11.26	-2.54	-9.87	-7.35
p_{OO}	-7.50	-5.49	-14.22	-1.26	2.38	1.28
p_{PBr}	1.01	-0.37	2.16	-0.15	0.47	1.92
p_{PC}	-0.31	2.68	1.14	7.88	0.63	2.73
p_{PH}	4.74		8.32		1.51	4.58
p_{PN}	-3.43	-11.54	-2.99	-7.18	-7.29	-7.44
p_{PO}	-6.66	-13.20	-8.89	-10.43	-6.97	-7.35
p_{PP}	4.45	-9.04	9.30	-8.20	-2.53	0.26
$p_{\text{Cl}^*}^b$						-3.45
p_{NCl^*}						-3.66
p_{HCl^*}						-6.18
$p_{\text{Cl}^*\text{Cl}^*}$						6.64
N	40	110	33	56	62	102
MAD	0.97	1.95	1.05	1.08	1.05	1.23
rmsd	1.26	2.47	1.48	1.45	1.36	1.52

^a All values are in kcal/mol. ^b Cl^* refers to the formally neutral chlorine atom in CH_3Cl .

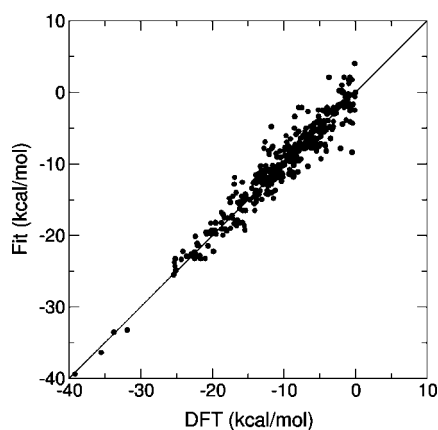


Figure 4. Isomerization energies computed using eq 8 versus the reference DFT values. The solid line corresponds to the function $y = x$.

parameters for oxidation states II and III of Ru and Os. The bond lengths for these metals in oxidation state III have larger errors; a detailed inspection of some of the worst cases revealed a marked Jahn–Teller distortion, particularly for Ru(III). This is expected for low-spin d^5

Table 3. Relative Energies of Compounds with Formula $[\text{Ir}(\text{H})(\text{PH}_3)(\text{NH}_3)_2(\text{OH}_2)\text{R}]^+$ (kcal/mol)

isomer	fit (eq 8)	DFT energy for ligand R				
		CH ₃ [−]	C ₂ H ₄ [−]	C ₆ H ₅ [−]	<i>p</i> -C ₆ H ₄ OMe [−]	<i>p</i> -C ₆ H ₄ NO ₂ [−]
1	−16.5	−15.7	−15.4	−14.1	−13.9	−14.3
2	−9.1	−9.3	−8.8	−8.6	−8.5	−8.6
3	−19.6	−20.9	−19.6	−20.5	−20.7	−20.1
4	−12.4	−13.4	−13.4	−10.3	−10.6	−12.9
5	−23.0	−23.4	−22.7	−22.2	−23.4	−23.4
6	−23.2	−22.5	−21.6	−21.0	−20.7	−21.0
7	0	0	0	0	0	0
8	−4.0	−3.9	−4.4	−3.8	−3.9	−3.9
9	−19.8	−20.1	−20.8	−19.5	−19.7	−19.2

Table 4. Parameters and Average Errors for the Bond Lengths Calculated Using Eq 6

parameter	Ru(II)	Ru(III)	Os(II)	Os(III)	Rh(III)	Ir(III)
r_{Br}^0 (Å)	2.543	2.396	2.566	2.414	2.448	2.363
r_{C}^0	2.084	2.062	2.020	2.064	2.048	2.011
r_{Cl}^0	2.425	2.283	2.430	2.307	2.362	2.298
$r_{\text{Cl}^*}^0$						2.252
r_{H}^0	1.565	1.553	1.567	1.586	1.510	1.484
r_{N}^0	2.114	2.087	2.081	2.087	2.060	1.954
r_{O}^0	2.159	2.081	2.140	2.068	2.102	1.977
r_{P}^0	2.272	2.237	2.219	2.242	2.242	2.151
s_{Br}	0.83	0.85	0.78	1.00	1.16	1.22
s_{C}	1.31	0.32	2.33	0.45	0.76	0.74
s_{Cl}	1	1	1	1	1	1
s_{Cl^*}						1.69
s_{H}	1.55	0.74	2.00	0.75	1.11	1.11
s_{N}	1.70	0.92	2.14	0.97	1.41	1.50
s_{O}	1.80	1.31	2.00	1.52	1.62	1.73
s_{P}	1.04	1.31	1.60	0.97	1.33	1.14
i_{Br}	2.06	5.28	2.09	4.45	2.77	6.25
i_{C}	5.76	13.02	4.52	10.66	9.07	11.48
i_{Cl}	2.01	4.87	2.14	4.30	2.32	5.81
i_{Cl^*}						4.13
i_{H}	5.99	14.80	4.68	11.68	8.23	11.41
i_{N}	1.84	4.04	2.05	3.65	1.78	5.42
i_{O}	0.95	2.12	1.63	1.89	0.99	4.41
i_{P}	3.25	6.25	3.35	6.10	3.54	7.42
N	306	426	294	420	516	660
MAD (Å)	0.020	0.023	0.020	0.021	0.019	0.015
rmsd (Å)	0.027	0.032	0.026	0.029	0.027	0.022

complexes. The Jahn–Teller effect may also explain why the errors in the isomerization energies were largest for Ru(III) complexes.

An analysis of the deviations as a function of total charge revealed a small correlation. Adding a term $q \cdot p_M$ to eq 6, where p_M is a metal-dependent parameter and q is the total charge, reduces the overall MAD by 0.001 Å and the rmsd by 0.002 Å. Because the improvement due to considering the charge is modest, we decided to keep the original form of eq 6 for simplicity.

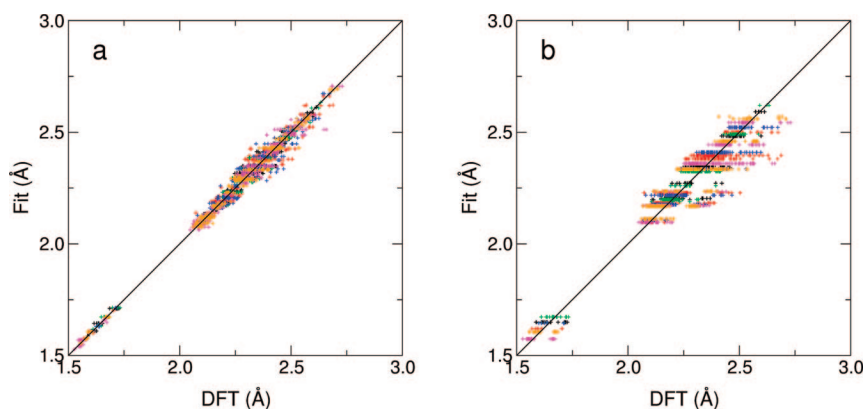


Figure 5. a) Bond lengths computed using eq 6 versus the reference DFT values. b) Fit to eq 6 neglecting the trans influence (i.e., $s_A = 0$ or $i_B = 0$). The solid lines correspond to $y = x$. Color code: black, Ru(III); red, Ru(IV); green, Os(II); blue, Os(III); magenta, Rh(III); orange, Ir(III).

Table 5. Relative Energies (in kcal/mol) for Complexes **1a–1d** from DFT, VALBOND-TRANS, and VALBOND Calculations

compound	DFT	VALBOND-TRANS		VALBOND	
		no charge	NPA	no charge	NPA
1a	8.6	7.5	7.1	−1.3	−2.0
1b	12.1	10.6	11.0	2.1	2.1
1c	0	0.0	0.0	0.0	0.0
1d	1.2	1.0	0.4	1.4	1.1

4. Application to Systems of Practical Relevance

To test the practicality of the method (referred to as VALBOND-TRANS), two series of complexes, the iridium dihydrides **1** and the monohydrides **2**, were investigated in more detail using DFT and VALBOND-TRANS. To this end, VALBOND and the extensions described above were implemented into CHARMM version 34a1.⁴³ The CHARMM22 parameter set was used.⁴³ When CHARMM force field parameters were missing, a) bond lengths were estimated as the sum of the covalent radii, and force constants were set to a default value; b) dihedrals were generally neglected, except for some dihedrals for triphenylphosphine and PHOX, which were obtained from energy scans on model compounds; c) partial charges were either set to zero or natural population analysis (NPA) charges from a DFT calculation were used;⁴⁴ and d) Lennard-Jones parameters were obtained from analogous CHARMM atom types. For simplicity, all angles, including those in the organic ligands, were treated using VALBOND, so no additional CHARMM angle bending parameters were necessary. All the nonstandard parameters that were used are listed in the Supporting Information.

As a first test, we revisited the iridium dihydrides involved in asymmetric hydrogenation, **1a–1d**, that we had studied previously.²⁴ The calculated DFT and VALBOND-TRANS energies are shown in Table 5. To assess the improvement due to the modifications presented in this work, the relative energies calculated using VALBOND without the trans terms are also shown. The qualitative stability sequence **1c** > **1d** > **1a** > **1b** is reproduced perfectly using VALBOND-TRANS, and the magnitudes of the relative energies are also reproduced well, with the largest deviation being 1.4 kcal/

mol, occurring for the highest-energy isomer. Without the trans term, the stability sequence is not reproduced, and the largest error increases to 10 kcal/mol. An important observation is that the difference between isomers **c** and **d** and between **a** and **b** can be assumed to be largely steric, because they both have the same pairs of trans ligands (e.g., for **c** and **d**, P is trans to Cl, N trans to H, and Cl trans to H). The steric energy difference is accounted for by the nonbonded (electrostatic and van der Waals) interactions in the CHARMM force field, which are represented using Coulomb's law and a Lennard-Jones potential. To test the influence of the partial charges on the results, the calculation was performed using two different charge models. In one, all the atoms had a partial charge of zero; in the other, the partial charges were set to the NPA charges from the B3LYP calculation on compound **1c**. The dielectric constant was set to $\epsilon = 4$, to account to some extent for the polarizability of the complex itself and for the large magnitude of the partial charges typical of the NPA method. Perhaps fortuitously, in this case the calculation with no charges agrees with the DFT results about as well as the calculation with the NPA charges.

As a second test, we considered complex **2**, which has been observed during the hydrogenation of imines using Ir-PHOX catalysts, as shown in Figure 6.⁴⁵ This complex has twenty possible diastereomers, which makes it an interesting test case. Again, the VALBOND-TRANS calculations were carried out using two different charge models, one with no charges and one with NPA charges, also with $\epsilon = 4$. To prevent the choice of a single reference isomer from biasing the evaluation of the average deviations, we considered the isomerization between each possible pair of isomers, for a total of 190 isomerization energies spanning a range from −20 to +20 kcal/mol. The mean absolute deviations between VALBOND-TRANS and DFT are 4.8 kcal/mol with no charges and 4.7 kcal/mol with NPA charges. The partial charges are largely configurationally independent; using the charges derived from any of the isomers produced similar results (not shown), which indicates that it is reasonable to use the same partial charges for every isomer. The results using NPA charges are shown in Figure 7a,c; the trend in isomerization energies is qualitatively correct but not within chemical accuracy and there are significant outliers. How-

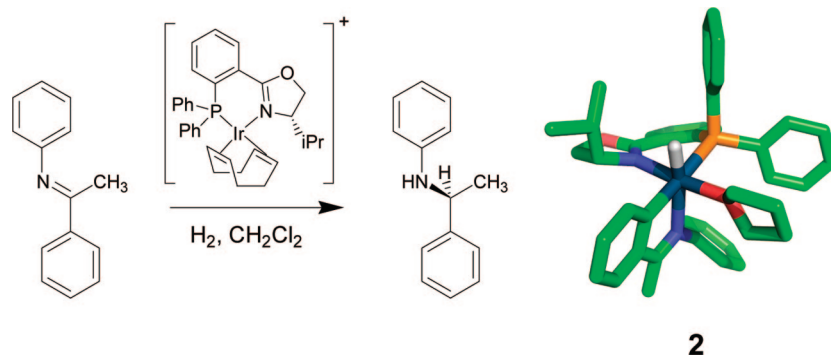


Figure 6. Catalytic imine hydrogenation, and structure of complex **2**, isolated when using THF as a solvent.

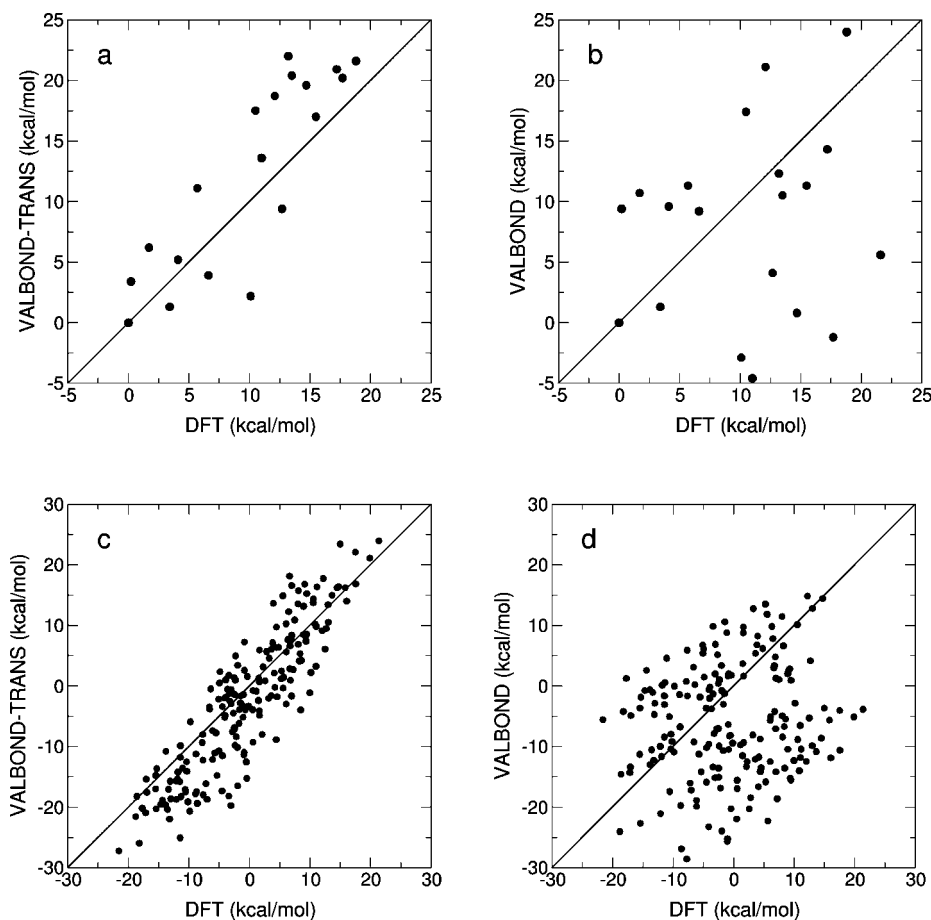


Figure 7. a) Relative energies of the 20 isomers of **2** using VALBOND-TRANS with NPA charges vs DFT. b) Same as a) but without including the new treatment of the trans influence. c) All isomerization energies between the 20 isomers of **2**, using VALBOND-TRANS vs DFT. d) Same as d) but without the trans influence. The solid lines correspond to the function $y = x$. The R^2 values for a-d are 0.78, 0.03, 0.79, and 0.02, respectively.

ever, the lowest-energy isomers are identified correctly using VALBOND-TRANS. When VALBOND without the trans terms is used instead, the low-energy isomers are not identified correctly and the correlation between the VALBOND and DFT energies is extremely poor, as shown in Figure 7b,d ($R^2 = 0.03$ and $\text{MAD} = 10.7$ kcal/mol). A calculation with $\epsilon = 1$ resulted in a mean absolute deviation of 10.8 kcal/mol, and an analysis of the energy terms indicated that the electrostatic repulsions were overestimated, overwhelming all the other energy terms. This special sensitivity to the electrostatic terms in the case of compound **2** may stem from its very crowded ligand environment.

The ability of the force field to reproduce the overall shape of the complexes was assessed qualitatively by superimposing the DFT- and VALBOND-TRANS-optimized structure that minimizes the rmsd (see Figure 8). A deviation that is noticeable in both cases is a slight difference in the twisting of the oxazoline ring as well as slightly different torsions for the phenyl rings. While such a measure is useful for visual comparison, the magnitude of the rmsd is, however, dominated by deviations of the more flexible parts away from the metal center. Therefore, a more direct comparison of the bond lengths and angles was made. Plots showing the correlation between the metal–ligand bond lengths using

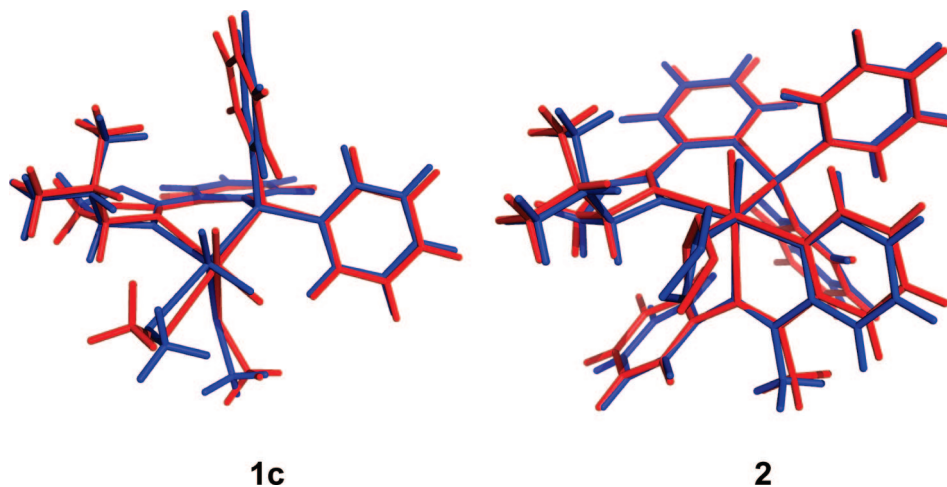


Figure 8. Comparison between the DFT-optimized structures (blue) and the VALBOND-TRANS-optimized structure (red) for compounds **1c** and the lowest energy isomer of **2**. The RMSDs are 0.53 Å and 0.34 Å, respectively; for discussion see text.

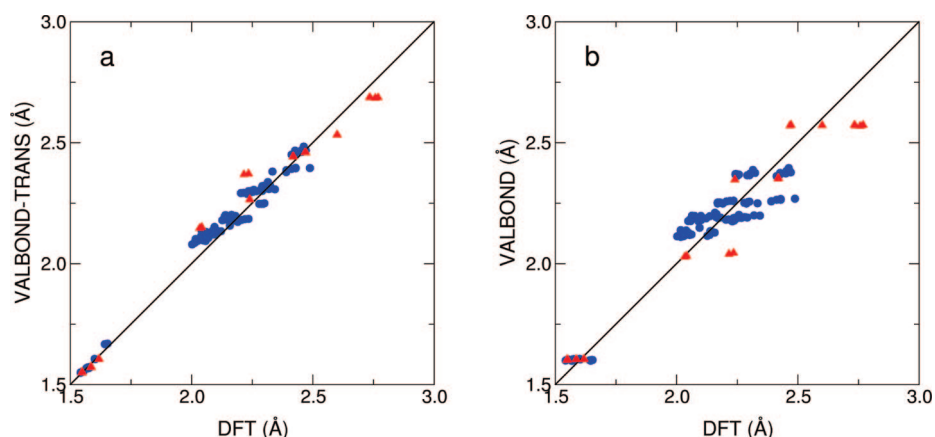


Figure 9. a) Bond lengths calculated using VALBOND-TRANS vs DFT for all isomers of compounds **1** (red triangles) and **2** (blue circles). b) Same as a) but without including the new treatment of the trans influence. The solid lines correspond to the function $y = x$.

VALBOND-TRANS and VALBOND vs DFT are shown in Figure 9. For both compounds **1** and **2**, the MAD for the bond lengths was 0.045 Å using VALBOND-TRANS, compared with 0.083 Å using VALBOND without the trans influence terms. For the angles, the MAD for compounds **1** and **2** were 6.4° and 4.0°, respectively, regardless of whether the trans influence terms were included or not. The largest deviations in the angles occur because normal sd^2 bending term in VALBOND is soft, while the hypervalent bending term in VALBOND is hard. As a result, large distortions such as the N–Ir–C angle, which is forced away from the ideal 90° due to the constraint of forming part of a five-member ring, have a large effect on the position of the trans atoms. For example, an N–Ir–H angle in the lowest energy isomer of **2** is 171.5° in the DFT geometry but 179.3° in the VALBOND geometry. Adjustment of the VALBOND parameters can reduce this problem, but for simplicity we decided to keep the default parameters in this work.

5. Conclusions

We have proposed and tested an extension of VALBOND combined with the CHARMM22 force field to account for the trans influence in octahedral complexes, based on

valence-bond concepts such as 3-center-4-electron bonds. The proposed function fits the 403 isomerization energies in the training set with a mean absolute deviation of 1.3 kcal/mol, a result which is close to chemical accuracy using a minimal number of atom types. We tested whether the resulting parameters are transferable to two series of related complexes with large chiral ligands. In the case of the dihydride complex **1**, VALBOND-TRANS reproduces the DFT results very well, while for compound **2** the results were more qualitative but still identified the most stable isomers correctly. This demonstrates that the force field allows for the separation of electronic and steric effects to investigate the stability of different diastereomers. Since the steric effect can be accounted for using traditional force field nonbonded terms, and it is the steric interactions with the chiral ligands which drive enantioselectivity, the proposed force field may become a powerful tool for the study of enantioselective reactions involving transition metal catalysts. There are several areas where further work will be beneficial: 1) the development of a fast and systematic way of determining the partial atomic charges, instead of using NPA charges from a DFT calculation; 2) the inclusion of Jahn–Teller distortions; 3) an extension of the method for pi and sigma

complexes, with ligands such as ethylene and H₂, respectively; 4) adiabatic reactive molecular dynamics, to potentially locate transition states; 5) extension to other metals and geometries; and 6) a more extensive reparametrization of the entire force field, including all relevant CHARMM and VALBOND parameters. The elements used in this work were chosen because of their importance to catalysis, the great stereochemical diversity allowed by the octahedral geometry, and their relatively simple electronic ground states. However, we expect that the method can be generalized to square-planar and trigonal bipyramidal geometries.

Acknowledgment. The authors thank the Swiss National Science Foundation for financial support. DFT calculations were carried out with a generous allocation of computing time on machines of the Swiss Center for Scientific Computing (CSCS), Manno, Switzerland. I.T.-B. was supported by a Marie Curie Fellowship (MIF1-CT2006-039088) from the European Commission.

Supporting Information Available: Tables of all the compounds in the training set and their DFT-computed energies and the nonstandard CHARMM parameters used in this work. This material is available free of charge via the Internet at <http://pubs.acs.org>.

References

- Strassner, T.; Taige, M. A. *J. Chem. Theory Comput.* **2005**, *1*, 848–855.
- Jorgensen, W. L.; Maxwell, D. S.; Tirado-Rives, J. *J. Am. Chem. Soc.* **1996**, *118*, 11225–11236.
- Weiner, S. J.; Kollman, P. A.; Case, D. A.; Singh, U. C.; Ghio, C.; Alagona, G.; Profeta, S.; Weiner, P. *J. Am. Chem. Soc.* **1984**, *106*, 765–784.
- Brooks, B. R.; Brucoleri, R. E.; Olafson, B. D.; States, D. J.; Swaminathan, S.; Karplus, M. *J. Comput. Chem.* **1983**, *4*, 187–217.
- Freddolino, P. L.; Arkhipov, A. S.; Larson, S. B.; McPherson, A.; Schulten, K. *Structure* **2006**, *14*, 437–449.
- Comba, P.; Remenyi, R. *Coord. Chem. Rev.* **2003**, *238*, 239, 9–20.
- Boeyens, J. C. A.; Comba, P. *Coord. Chem. Rev.* **2001**, *212*, 3–10.
- Comba, P.; Zimmer, M. *J. Chem. Educ.* **1996**, *73*, 108–110.
- Bernhardt, P. V.; Comba, P. *Inorg. Chem.* **1992**, *31*, 2638–2644.
- Comba, P. *Coord. Chem. Rev.* **1993**, *123*, 1–48.
- Landis, C. R.; Root, D. M.; Cleveland, T. *Rev. Comput. Chem.* **1995**, *6*, 73–148.
- Zimmer, M. *Chem. Rev.* **1995**, *95*, 2629–2649.
- Norrby, P. O.; Brandt, P. *Coord. Chem. Rev.* **2001**, *212*, 79–109.
- White, D. P.; Douglass, W. *Molecular Mechanics Modeling of Organometallic Catalysts*. In *Computational Organometallic Chemistry*; Cundari, T. R., Ed.; Marcel Dekker: 2001; pp 237–274.
- Donoghue, P. J.; Helquist, P.; Norrby, P.-O.; Wiest, O. *J. Chem. Theory Comput.* **2008**, *4*, 1313–1323.
- Comba, P.; Zimmer, M. *Inorg. Chem.* **1994**, *33*, 5368–5369.
- Deeth, R. J. *Coord. Chem. Rev.* **2001**, *212*, 11–34.
- Danielsson, J.; Meuwly, M. *J. Chem. Theory Comput.* **2008**, *4*, 1083–1093.
- Roseblade, S. J.; Pfaltz, A. *Acc. Chem. Res.* **2007**, *40*, 1402–1411.
- Lightfoot, A.; Schnider, P.; Pfaltz, A. *Angew. Chem., Int. Ed. Engl.* **1998**, *37*, 2897–2899.
- Pfaltz, A.; Blankenstein, J.; Hilgraf, R.; Hormann, E.; McIntyre, S.; Menges, F.; Schonleber, M.; Smidt, S. P.; Wustenberg, B.; Zimmermann, N. *Adv. Synth. Catal.* **2003**, *345*, 33–44.
- Kaellstroem, K.; Munslow, I.; Andersson, P. G. *Chem. Eur. J.* **2006**, *12*, 3194–3200.
- Cui, X.; Burgess, K. *Chem. Rev.* **2005**, *105*, 3272–3296.
- Mazet, C.; Smidt, S. P.; Meuwly, M.; Pfaltz, A. *J. Am. Chem. Soc.* **2004**, *126*, 14176–14181.
- Root, D. M.; Landis, C. R.; Cleveland, T. *J. Am. Chem. Soc.* **1993**, *115*, 4201–4209.
- Cleveland, T.; Landis, C. R. *J. Am. Chem. Soc.* **1996**, *118*, 6020–6030.
- Landis, C. R.; Cleveland, T.; Firman, T. K. *J. Am. Chem. Soc.* **1998**, *120*, 2641–2649.
- Rappe, A. K.; Casewit, C. J.; Colwell, K. S.; Goddard, W. A., III; Skiff, W. M. *J. Am. Chem. Soc.* **1992**, *114*, 10024–10035.
- Piquemal, J.-P.; Williams-Hubbard, B.; Fey, N.; Deeth, R. J.; Gresh, N.; Giessner-Prettre, C. *J. Comput. Chem.* **2003**, *24*, 1963–1970.
- Deeth, R. J. *Inorg. Chem.* **2007**, *46*, 4492–4503.
- Pidcock, A.; Richards, R. E.; Venanzi, L. M. *J. Chem. Soc. A* **1966**, 1707, 1710.
- Coe, B. J.; Glenwright, S. J. *Coord. Chem. Rev.* **2000**, *203*, 5–80.
- Steele, W. V. *Annu. Rep. Prog. Chem., Sect. A Inorg. Chem.* **1975**, *71*, 103–118.
- Brandt, P.; Norrby, T.; Aakermark, B.; Norrby, P.-O. *Inorg. Chem.* **1998**, *37*, 4120–4127.
- Weinhold, F.; Landis, C. R. *Valency and Bonding: A Natural Bond Orbital Donor-Acceptor Perspective*; Cambridge University Press: 2005; pp 473–474.
- Harvey, J. N.; Heslop, K. M.; Orpen, A. G.; Pringle, P. G. *Chem. Commun. (Cambridge, U.K.)* **2003**, 278, 279.
- Pearson, R. G. *Inorg. Chem.* **1973**, *12*, 712–713.
- Allen, F. H. *Acta Crystallogr., Sect. B: Struct. Sci.* **2002**, *58*, 380–388.
- Becke, A. D. *J. Chem. Phys.* **1993**, *98*, 5648–5652.
- Frisch, M. J.; Trucks, G. W.; Schlegel, H. B.; Scuseria, G. E.; Robb, M. A.; Cheeseman, J. R.; Montgomery, J. A., Jr.; Vreven, T.; Kudin, K. N.; Burant, J. C.; Millam, J. M.; Iyengar, S. S.; Tomasi, J.; Barone, V.; Mennucci, B.; Cossi, M.; Scalmani, G.; Rega, N.; Petersson, G. A.; Nakatsuji, H.; Hada, M.; Ehara, M.; Toyota, K.; Fukuda, R.; Hasegawa, J.; Ishida, M.; Nakajima, T.; Honda, Y.; Kitao, O.; Nakai, H.; Klene, M.; Li, X.; Knox, J. E.; Hratchian, H. P.; Cross, J. B.; Bakken, V.; Adamo, C.; Jaramillo, J.; Gomperts, R.; Stratmann, R. E.; Yazyev, O.; Austin, A. J.; Cammi, R.; Pomelli, C.; Ochterski, J. W.; Ayala, P. Y.; Morokuma, K.; Voth, G. A.

- Salvador, P.; Dannenberg, J. J.; Zakrzewski, V. G.; Dapprich, S.; Daniels, A. D.; Strain, M. C.; Farkas, O.; Malick, D. K.; Rabuck, A. D.; Raghavachari, K.; Foresman, J. B.; Ortiz, J. V.; Cui, Q.; Baboul, A. G.; Clifford, S.; Cioslowski, J.; Stefanov, B. B.; Liu, G.; Liashenko, A.; Piskorz, P.; Komaromi, I.; Martin, R. L.; Fox, D. J.; Keith, T.; Al-Laham, M. A.; Peng, C. Y.; Nanayakkara, A.; Challacombe, M.; Gill, P. M. W.; Johnson, B.; Chen, W.; Wong, M. W.; Gonzalez, C.; Pople, J. A. *Gaussian 03, Revision B.01*.
- (41) Glendening, E. D.; Reed, A. E.; Carpenter, J. E.; Weinhold, F. *NBO Version 3.1*.
- (42) Hay, P. J.; Wadt, W. R. *J. Chem. Phys.* **1985**, *82*, 270–283.
- (43) MacKerell, A. D., Jr.; Bashford, D.; Bellott, M.; Dunbrack, R. L.; Evanseck, J. D.; Field, M. J.; Fischer, S.; Gao, J.; Guo, H.; Ha, S.; Joseph-McCarthy, D.; Kuchnir, L.; Kuczera, K.; Lau, F. T. K.; Mattos, C.; Michnick, S.; Ngo, T.; Nguyen, D. T.; Prodhom, B.; Reiher, W. E., III; Roux, B.; Schlenkrich, M.; Smith, J. C.; Stote, R.; Straub, J.; Watanabe, M.; Wiorkiewicz-Kuczera, J.; Yin, D.; Karplus, M. *J. Phys. Chem. B* **1998**, *102*, 3586–3616.
- (44) Reed, A. E.; Weinstock, R. B.; Weinhold, F. *J. Chem. Phys.* **1985**, *83*, 735–746.
- (45) Barrios-Landeros, F.; Pfaltz, A. Ir-catalyzed enantioselective hydrogenation of imines: Catalytic intermediates and mechanistic study. Presented at the 23rd International Conference on Organometallic Chemistry, Rennes, France, 2008.

CT800392N